Scaling Relation between Current through Suspensions of Carbon-doped Nanoporous TiO_2 Submicron Particles in Silicone Oil and Reciprocal of Shear Rate under Combined Electric and Shear Fields

Z.Y. Qiu[*], Y. Shen[**], L.W. Zhou[***] and Y.H. Zhu[****]

[*]Fudan University, Department of Physics, Shanghai 200433, China
[*]The City College of New York, New York, NY10031, USA, ltscltsc@hotmail.com
[**]Zhengzhou University of Light Industry, Zhengzhou 450002, China, hnshenyan@126.com
[***]Fudan University, Department of Physics, Shanghai 200433, China, lwzhou@fudan.edu.cn
[****]East China University of Science and Technology, Shanghai 200237, China, yhzhu@ecust.edu.cn

ABSTRACT

We experimentally demonstrate that there is a simple scaling relation between DC current through a suspension of carbon-doped nanoporous TiO_2 submicron particles in silicone oil and reciprocal of shear rate under combined DC electric and shear fields in a rotating coaxial stainless steel cylinder rheometer. Carbon-doped TiO_2 powder is synthesized by hydrolysis of $Ti(OBu)_4$ in alcoholic solution and dodecylamine (DDA) acts as a template. Synthesized carbon-doped TiO_2 powder is carbonized at 673ºK under protection of flowing N_2 gas. Carbon-doped nanoporous TiO_2 submicron particles are quantitatively characterized by TEM, XRD, XPS and other analysis tools. The particle size distribution is 100 to 200nm. There are 4~6nm pores on the particle surface layer. The carbon is distributed in a thin 6nm thin surface layer of the particle. An application of the particles is suggested.

***Key Words*:** scaling relation, shear rate, current density, carbon-doped nanoporous TiO_2 submicron particle

1 INTRODUCTION

The preparation or modification of property-adjustable composite nanoparticles has important scientific and industrial applications. The common goal is to develop low cost techniques to synthesize or modify nanoparticles for a diverse range of uses in different fields. Quantitative characterization provides a basis for understanding structures, properties and functions of nanoparticles as well as their mutual interactions. This is of critical importance in their synthesis and applications. In particular, TiO_2 powder plays a critical role. Our initial motivation for this work was to enhance conductivity of TiO_2 powders [1] and so change its dielectric response rate by chemically inserting carbon into TiO_2 crystalline structures [2][3]. Unexpectedly, we have found other properties and functions of the carbon-doped nanoporous TiO_2 submicron particles which have potential application in areas that we had not anticipated. This report will focus on one of our findings that there is a scaling relation between DC current density through a suspension of the particles in silicone oil and the reciprocal of shear rate. This paper discusses synthesis, processing and characterization of the particles, and concludes with a suggested application of the particles for separation of guest particles.

2 SUBMICRON PARTICLE PREPARATION

2.1 Synthesis and Processing

Carbon-doped TiO_2 powder is synthesized by hydrolysis of tetra-n-butyl titanate $Ti(OBu)_4$ in alcoholic solution and dodecylamine (DDA) acts as a template. The amount of DDA controls the carbon content of the final product. The amount of DDA is varied from 0 to 270g and uniformly mixed with 100ml of $Ti(OBu)_4$ in a flask. 350ml of ethanol and 50ml of deionized water are quickly added to the above mixture. The resulting mixture is continuously stirred for two hours at 350ºK. The product is isolated by vacuum filtration and then dried in air at 350ºK overnight.

The carbonization of the synthesized TiO_2 powder is key to the quality of the final product. The initial temperature ramp rate has significant effect on the dispersion of the particles. The carbonization temperature and time determine the carbon content of the final product. The powder is carbonized in a sealed quartz tube oven with a pair of inlet and outlet openings for protective nitrogen gas. The carbonization has three steps. First, the TiO_2 powder is loaded into the oven and the oven temperature is increased from the room temperature to 383ºK , 673ºK or 873ºK within 80~120minutes. Then, the powder is kept in the oven at one of these three temperatures for 8 hours. Finally the powder is cooled down to room temperature. During the carbonization, the powder is protected by N_2 gas flowing into the oven through the inlet. The carbonized powder is kept in a dry box at 393ºK. Based on our tests, the powder is best carbonized at 673ºK for 8 hours. The best DDA/TiO_2 molar ratio for the reaction falls in the range 0.046~0.092. All the samples of TiO_2 powders are carbonized at 673ºK unless otherwise specified. The final product is well dispersed carbon-doped nanoporous TiO_2 submicron particles.

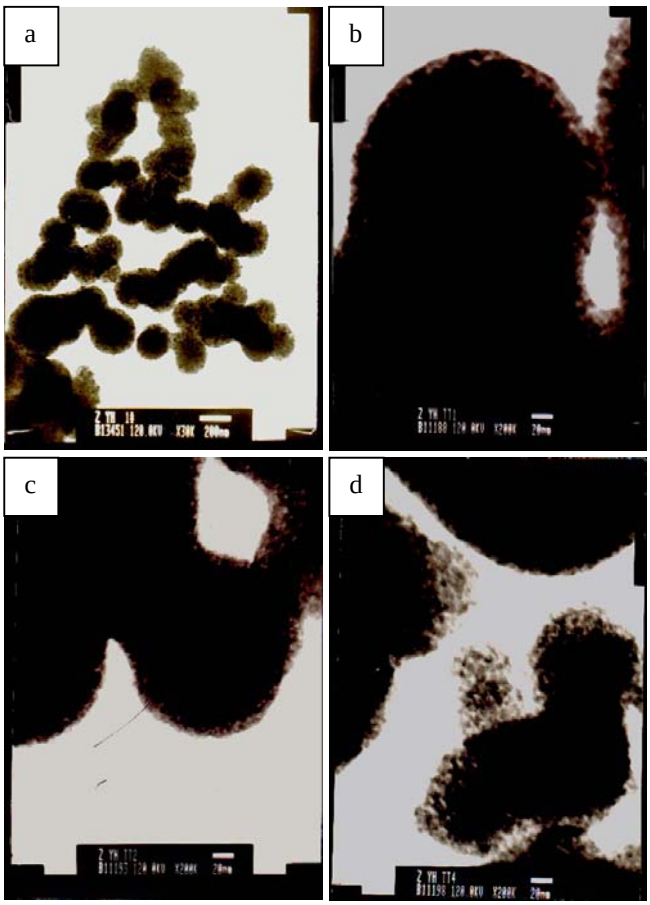

Figure 1: TEM images of Samples 1, 2 and 3.

2.2 Characterization

The size distribution and morphology of carbon-doped nanoporous TiO_2 submicron particles are deter-mined by TEM images of the three samples obtained from a transmission electron microscopy (Jeol JEM 1200EX), see Figure 1. The DDA/TiO_2 molar ratio of Sample 1 is 0.046; its TEM image is shown in Figure 1(a) and its higher resolution image in Figure 1(b). The particle size distribution of Sample 1 is from 80 to 130nm with an average size of 102nm, and most particles are almost spherical. The DDA/TiO_2 molar ratio of Sample 2 is 0.092 and its TEM image is shown in Figure 1(c). The DDA/TiO_2 molar ratio of Sample 3 is 0.600 and its TEM image is shown in Figure 1(d). There are clearly visible pores with diameters that range from 4 to 6nm on the submicron particle surface layer, as shown in Figures 1(b)(c)(d).

Data for the isotherms of N_2 adsorption-desorption of Sample 1 and Sample 2 are collected at 77.35ºK on a micromeritics ASAP 2010 analyzer. Each sample is activated at 523ºK in a vacuum for fifteen hours before data acquisition. The N_2 adsorption-desorption isotherms of Sample 1 and 2 are shown in Figure 2. Based on IUPAC [4], both the isotherms are classified as type IV. The two observed hysteresis loops (type H1) within the relative

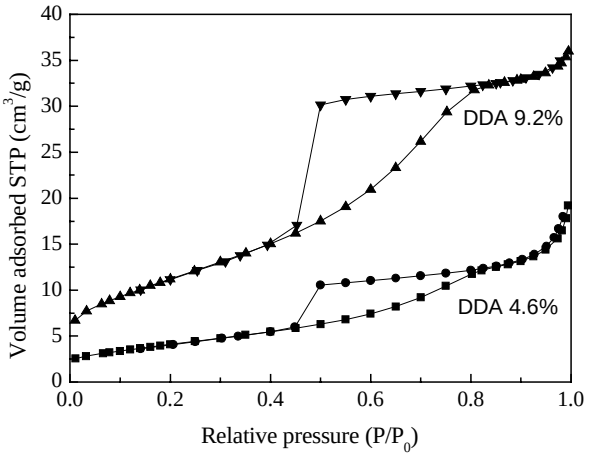

Figure 2: N_2 adsorption-desorption isotherms for Sample 1 and Sample 2.

pressure of 0.45 to 0.8 are direct evidence of the constriction of nanoporous structures in the two samples [5]. The method of Barrett-Joyner-Halenda (BJH) is used to estimate the BET surface area of a sample. Sample 1 has a BET surface area of 15.0 m^2/g and an average pore size of 6.0nm. Sample 2 has a BET surface area of 41.0 m^2/g and the average pore size of 4.4nm. The BET surface area of the particles increases with the DDA content. The higher the DDA content, the higher the porosity of the particles after the carbonization.

X-ray diffraction (XRD) data for Sample 2 are collected on a Rigagu D/max-rB diffratometer. The X-ray used is the nickel-filtered Cu's Kα ray with a wavelength of 1.5406 Å. Shown in Figure 3 are the XRD patterns for Sample 2. The XRD peaks show that there are combined anatase and rutile structures in Sample 2. These peaks are broad. The Williamson-Hall method [6] is used to estimate the lattice distortion of Sample 2. The distortion is negligible. The broad XRD peaks are caused by the decrease of the TiO_2 crystallite size when carbon is chemically inserted into the TiO_2 crystalline structures. The conventional Scherre's method is used to estimate the grain size of Sample 2. This is 11.96nm and is larger than the pore size.

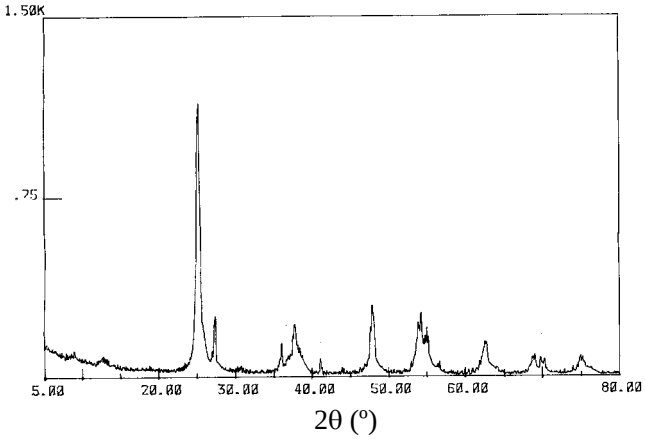

Figure 3: XRD patterns for Sample 2. The vertical axis is a relative intensity of diffracted X-ray.

The carbon content of Sample 2 is measured as 2.6% by weight by a MOD 1106 elemental analyzer. The XPS data show that carbon is distributed in a thin 6nm surface layer of particles.

3 CURRENT SCALING RELATIONS

3.1 Setup Description

The dynamic current measurement system consists of four units: (1) a servo-motor, (2) a servo-motor drive and control unit, (3) a stainless steel coaxial cylindrical rheometer with a uniform gap of 0.5mm as a sample cell for the dynamic current measurement. The inner and outer cylinders are electrically insulated that act as a pair of electrodes, and (4) a current sampling and data acquisition unit. The core unit is the sample cell and the challenge is to keep the gap between the two cylinders uniform within a design tolerance of 1% when the inner cylinder is driven or rotated at a rotational speed of 0.1 to 3000RPM. All the units are adjusted to meet this challenge. First, we use a pair of high precision bearings to secure the rotator of the inner cylinder with a tolerance of 3μm. Second, the inner surfaces of the cell are milled to have a roughness of 1~3μm. Third, based on its torque-velocity-voltage curves, the servo-motor is set to work in the most stable mode. Fourth, the driving and control unit are set to work in the gentlest acceleration mode. Finally, a soft connection between the driving and rotator shafts further reduces the negative influence of the driving force on the gap uniformity. The multiple brass brushes surrounding the rotator shaft reduce the current noise to negligible levels. The output fluctuation of the high voltage DC power supply is 0.1% and the tolerance of the sampling resistor used is 0.1%.

The gap uniformity has been cross-checked by different methods. First, the static capacitance of the empty cell is measured with a LCR meter (HP 4284A) at the frequencies from 10Hz to 1MHz. Second, a similar measurement is performed when the rotator is rotated at a speed from 0.1 to 3000RPM. The difference limit of the static and dynamic capacitance of the empty gap is 1%. Third, the gap is filled with paraffin oil, and the static and dynamic capacitance of the sample cell is measured with the same LCR meter. The difference limit is still ~ 1%. Finally, paraffin oil is replaced with silicone oil. The above measurements are repeated. The largest difference of the static and dynamic capacitance is still 1%. The working voltage of the RCL meter is 1V/10Hz~1MHz for all the above measurements. Also, we check the difference of the static and dynamic capacitance under a high AC voltage of 100~1000V/40~2000Hz with a high voltage AC electric bridge. All the low-voltage measurements of static and dynamic capacitance of the sample cell are repeated on the high voltage electric bridge. The upper limit of the difference between the static and dynamic capacitance of the sample cell is 1% when the sample cell is filled with air, paraffin oil or silicone oil. Thus, a reasonable estimate of a total error of the dynamic current data is < 2% in the ranges of shear and electric fields of interest.

3.2 Current Scaling Relations

Sample 1 is uniformly dispersed into silicone oil to form a suspension at 10% by weight with help of an ultrasound bath. The suspension is loaded into the sample cell. Shear rate (D) is calculated based on rotational speed and dimensions of the cell. For a fixed electric field and rotational speed, current data are collected when both the rotation and the current are stable. The rotational speed is then changed, and the current data collected again when both the rotation and the current become stable. Our dynamic current data cover shear rates from 3.8 to 3587.4 1/s and direct electric fields from 10 to 1200V/mm. All the current density data at the fixed electric fields are plotted against the reciprocal of shear rate (1/D) in Figure 4. The data clearly demonstrate that there are scaling relations between the DC current density and the reciprocal of shear rate within 2~4 orders of the experimental parameters of the shear rate, electric field strength and the current density. We curve fit the current data for each electric field using the relation log J = A + B log (1/D) where A and B are two electric field dependent coefficients, shown in Figure 5. In addition, we calculate the correlation coefficient for each set of current data for each electric field strength, shown in Figure 6. When the electric field > 200V/mm, the correlation coefficient is almost 1. The high correlation of the current data for all fixed electric field strengths confirms the scaling relation between the current and the reciprocal of shear rate. Let's take a close look at the current curves in Figure 4. There is a concave-convex transition of the curves from the lower to higher electric field strengths. This is reflected in the curves of the correlation coefficients versus electric field strength in

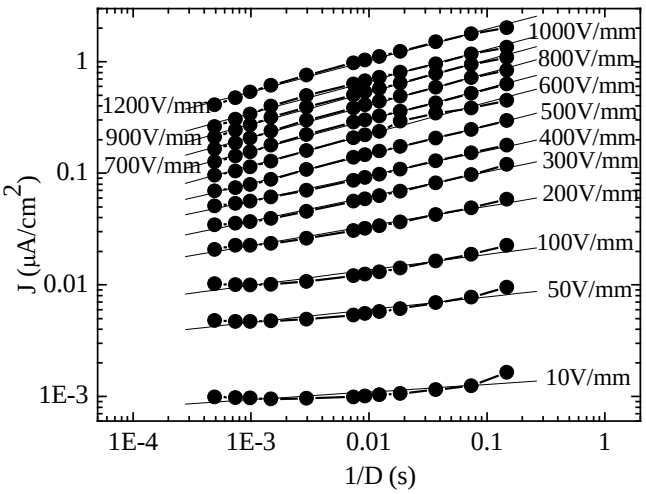

Figure 4: A scaling relation between the current density (J) through a suspension of Sample 1 in silicone oil and the reciprocal of shear rate (1/D) for fixed electric fields.

NSTI-Nanotech 2007, www.nsti.org, ISBN 1420061844 Vol. 3, 2007

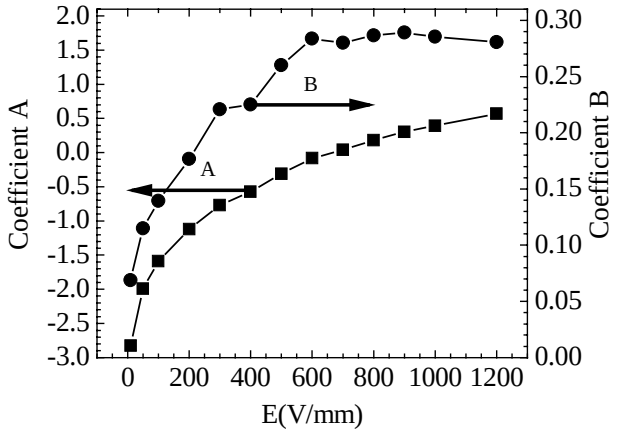

Figure 5: Coefficients of A and B versus electric field

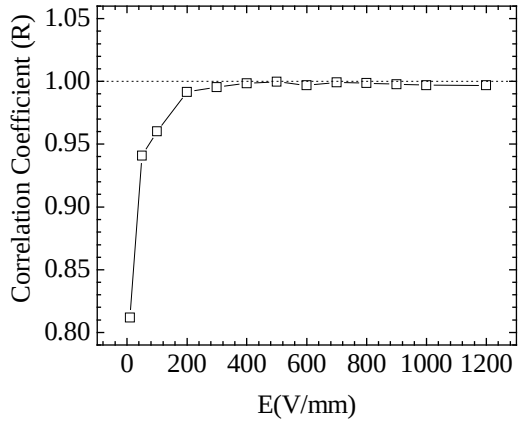

Figure 6: Correlation coefficient (R) versus electric field

Figure 5. The critical electric field is 500V/mm at which the correlation coefficient is 0.9995, closest to 1 and all the current data fall on a straight line. For the higher electric fields, the correlation coefficient decreases slightly.

An intuitive physical picture is that a DC electric field induces particle chain formation while a shear field destroys existing particle chains and prevents chain formation. The conductivity of silicone oil is negligible compared with that of the carbon-doped submicron particles. Particle chain formation favors current increase while the shear field causes chain fragmentation, and so leads to a current decrease. It is the most unusual that the current at different stable rotation speeds and the reciprocal of the shear rate are related by a simple scaling relation. One explanation is that self-similar structures are created in the suspension and this leads to a simple scaling relation. What would cause self-similar structures to form has to be investigated. A hybrid MD-continuous model is being developed to numerically simulate particle configurations under different electric and shear fields. Limited data from preliminary numerical simulations suggest that chains seem to be broken, re-built and re-attached to other chain segments *spatially at random*. It is hard to predict whether chains stay or slip on the electrode surface and why.

4 CONCLUSIONS AND FUTURE WORK

We experimentally demonstrate that there is a scaling relation between the DC current through the suspension of carbon-doped nanoporous TiO_2 submicron particles in silicone oil and the reciprocal of shear rate when DC electric and shear fields are varied. The well dispersed carbon-doped nanoporous TiO_2 submicron particles are prepared by hydrolysis of $Ti(OBu)_4$ with DDA acting as template and carbonization at 673K. The final product is characterized by a N_2 adsorption-desorption isotherm, TEM, XRD, XPS and an element analyzer. The particles size distribution varies from 100 to 200nm and the pore size on the particle surface layer is 4 to 6nm. According to the XPS analyses, carbon is distributed in a thin 6nm surface layer of particles.

In the future, we will continue to improve the hybrid MD-continuous model for particle chain dynamics under combined electric and shear fields. With help of numerical simulations, we will attempt to explain the current scaling relation. In addition, one application of the particles for separation of guest particles is proposed below. The relative dielectric constant of the TiO_2 particles is adjusted to 80 by an AC electric field frequency or other way, which matches that of water. Induced by a DC or/and AC electric field(s), the particles will form particle chains in de-ionized water. These particle chains would be 'dielectrically' transparent. Between a particle core and water, there is a 6nm thick carbon-doped spherical shell. So guest particles leaving or approaching to the TiO_2 host particles could be monitored. Some experiments will be designed based on this idea.

The work was supported by the NSF of China under Grant Nos. 1983402 and 19774019. The authors sincerely thank Professor S. Weinbaum for his critical comments on the manuscript. One of the authors (ZYQ) thanks Professor S. Fritton for her critically reading the first manuscript, thanks Dr S. Tada for his helpful suggestions in numerical simulations, and thanks Mr. J. Ma for his comments and generous help in preparing the manuscript. Finally, Z.Y. Qiu gratefully acknowledges the support from PSC-CUNY Professional Development Fund.

REFERENCES

[1] Z.Y. Qiu, F.K. Shan, L.W. Zhou, F. Lu and Y.H. Zhu, International J. Mod. of Phys. B, 15, 618, 2001.
[2] J.E. Martin, R. A. Anderson, J. Odinek, D. Adolf and J. Williamson, Phys. Rev. B 67, 094207, 2003.
[3] J.E. Martin, C.P. Tigges, R.A. Anderson and J. Odinek, Phys. Rev. B 60, 7127, 1999.
[4] S. J. Gregg, K. S. W. Sing, Adsorption, Surface Area and Porosity, Academic Press, London, 1, 1995.
[5] M. Thieme, F. Schuth, Microporous Mesoporous Mater. 27, 193, 1999.
[6] G. K. Williamson, W. H. Hall, Acta Met. 1, 22, 1953.